The Search for Color Transparency at 12 GeV

July 7, 2006

J. Dunne and D. Dutta (Co-spokesperson and contact person)
MISSISSIPPI STATE UNIVERSITY

P. Bosted, A. Bruell, D. Gaskell, D.G. Meekins, R. Ent (Co-spokesperson,*),
H.C. Fenker, M.K. Jones, D. Higinbotham, T. Horn, D. Mack, G. Smith,
S.A. Wood, and W.F. Vulcan
JEFFERSON LAB, (*) and HAMPTON UNIVERSITY

I. Albayrak, M.E. Christy, C.E. Keppel (*), S. Malace, O.Oyebola,
H. Pushpakumari, V. Tvaskis, and L. Tang (*)
HAMPTON UNIVERSITY, (*) and JEFFERSON LAB

W. Chen, H. Gao, K. Kramer, X. Qian, Q. Ye, X. F. Zhu, X. Zong
DUKE UNIVERSITY

G.M. Huber
UNIVERSITY OF REGINA

A. Asaturyan, A. Mkrtchyan, H. Mkrtchyan, T. Navasardyan, V. Tadevosyan
YEREVAN PHYSICS INSTITUTE

Abstract

We propose to measure the A(e,e'p) proton knockout and the A(e,e'π^+) pion electroproduction cross sections to extract the proton and the pion nuclear transparencies in the nuclear medium. We restrict the proton transparency measurements to the ^{12}C nucleus with additional ^{1}H measurements (to determine the elementary process), over the range Q^2 = 8 - 16 (GeV/c)^2. The pion (π^+) transparency measurements will be performed on ^{1}H, ^{2}H, ^{12}C, and ^{63}Cu, over the range Q^2 = 5 - 9.5 (GeV/c)^2. A rise in the pion and proton transparency as a function of Q^2 is predicted to be a signature of the onset of Color Transparency. For the latter measurements, with a less known reaction mechanism, it is essential to map both the Q^2- and A-dependence.

Recent experiments have reported evidence for Color Transparency effects at $Q^2 \simeq 10$ (GeV/c)^2. This is further corroborated by hints of such effects seen at lower Q^2 in pion photo- and electro-production from nuclei. Unambiguous observation of Color Transparency would uniquely point to the role of color in exclusive high-Q^2 processes. In addition, the occurrence of such effects is an effective signature of the approach to the factorization regime in meson electroproduction experiments, necessary for the access to Generalized Parton Distributions. The proposed experiment seeks to measure the pion and proton transparencies up to the highest Q^2 that can easily be reached at a 12-GeV JLab, using the HMS and SHMS spectrometers. We request a total of 26 days of beamtime with a beam current of 80μA.

Contents

1 Technical Participation of Research Groups

1.1 Mississippi State University

One spokesperson is part of the Mississippi State University group. The MSU groups intends to take responsibility for the design and commissioning of the collimator and sieve-slit mechanism for the SHMS spectrometer. The MSU group also will develop a TRD detector program (not part of the baseline equipment) for the SHMS.

1.2 Hampton University

The co-spokesperson is part of the Hampton University group. The Hampton University group intends to be part of a collaboration to seek NSF funding for the drift chambers for the SHMS. They will take responsibility for the construction of the wire chambers for the SHMS spectrometer.

1.3 Yerevan Physics Institute

The Yerevan group is actively involved in this proposal and this group intends to design and build the lead-glass calorimeter for the SHMS, and be instrumental in obtaining the lead-glass calorimeter blocks for this detector.

2 Physics Motivation

2.1 Overview

The quarks and gluons of QCD are hidden. Protons and neutrons that are the constituents of nuclei are identified with color singlet states and have strong interactions very different from that of the gluon exchange by colored quarks and gluons. Protons and neutrons rather seem bound together by the exchange of evanescent mesons. Hence, at low energies or long distances the nucleon-meson picture in the standard model of nuclear physics is very successful in describing the overall features of the strong interaction. Nonetheless, at sufficiently high energies or short distances perturbative QCD (pQCD) with its quark-gluon degrees of freedom must allow for extremely precise description of nuclei. Unfortunately, there is no clear understanding of how these two regimes are connected. The study of the transition between these regimes, transcending from the hadronic degrees of freedom to the partonic degrees of freedom is an important goal in intermediate energy nuclear and particle physics.

The availability of high-energy beams provides the opportunity to search for the presence of QCD as the ultimate source of the strong interaction. In particular, exclusive and semi-exclusive processes are essential in studies of the role of color in high-momentum transfer processes. This is because manifestation of the underlying quark-gluon degrees of freedom of QCD naturally gives rise to a distinct set of phenomena in exclusive processes on nucleons and nuclei. A popular method, then, used to explore the transition region is to look for the onset of such phenomena. One such fundamental prediction of

QCD is the phenomenon of Color Transparency (CT), that refers to the vanishing of the final (and initial) state interactions of hadrons with the nuclear medium in exclusive processes at high momentum transfer [1].

The concept of Color Transparency (CT) was introduced two decades ago by Mueller and Brodsky [1], and since has stimulated great experimental and theoretical interest. CT is an effect of QCD, related to the presence of non-abelian color degrees of freedom underlying strongly interacting matter. The basic idea is that, under the right conditions (such as sufficiently high momentum transfer), three quarks, each of which would normally interact very strongly with nuclear matter, could form an object of reduced transverse size, (i.e. scattering takes place via selection of amplitudes in the initial and final state hadrons characterized by a small transverse size). Secondly, this small object should be 'color neutral' outside of this small radius in order not to radiate gluons. Finally, this compact size must be maintained for some distance in traversing the nuclear medium, so that it passes undisturbed through the nuclear medium. A similar phenomenon occurs in QED, where an e^+e^- pair of small size has a small cross section determined by its electric dipole moment [2]. In QCD, a $q\bar{q}$ or qqq system can act as an analogous small color dipole moment.

CT was first discussed in the context of perturbative QCD. Later works [3] have indicated that this phenomenon also occurs in a wide variety of models which feature non-perturbative reaction mechanisms. Unambiguous observation of CT would provide a new means to study the strong interaction in nuclei and it would be a clear manifestation of hadrons fluctuating to a small size in the nucleus. Moreover, it also contradicts the traditional Glauber multiple scattering theory in the domain of its validity. Nuclear transparency defined as the ratio of the cross section per nucleon for a process on a bound nucleon in the nucleus to the cross section for the process on a free nucleon, is the commonly used observable in searches for this phenomena. Therefore, measurements of nuclear transparency have attracted a significant amount of effort over the last two decades. A clear signature for the onset of CT would involve a dramatic rise in the nuclear transparency as a function of momentum transfer involved in the process, i.e. a positive slope with respect to the momentum transfer.

More recently, CT has also been discussed in the context of QCD factorization theorems. These factorization theorems were, over the last few years, derived for various deep inelastic exclusive processes [4, 5, 6, 7], and are intrinsically related to the access to Generalized Parton Distributions (GPD's), introduced by Ji and Radyushkin [8, 9]. The discovery of these GPD's and their connection to certain totally exclusive cross sections has made it possible in principle to rigorously map out the complete nucleon wave functions themselves. The GPD's contain a wealth of information about the transverse momentum and angular momentum carried by the quarks in the proton. Presently, experimental access to such GPD's is amongst the highest priorities in intermediate energy nuclear/particle physics.

It is still uncertain at which Q^2 value one will reach the factorization regime, where leading-order perturbative QCD is fully applicable. It is expected to be between $Q^2 =$ 5 and 10 $(\mathrm{GeV/c})^2$ for meson electroproduction. For example, it is generally believed that the pion elastic form factor is dominated by long-distance confinement-based physics for $Q^2 < 10$ $(\mathrm{GeV/c})^2$. Nonetheless, Eides, Frankfurt, and Strikman [10] point out that

"It seems likely that a *precocious factorization* ... could be valid already at moderately high Q^2 [$\geq$ 5 (GeV/c)^2], leading to precocious scaling of the spin asymmetries and of the ratios of cross sections as function of Q^2 and x". On the other hand if higher-twist contributions such as quark transverse momentum contributions are appreciable (they are predicted to be a factor of $\approx$ 2-3, for $Q^2 \approx$ 3-10 (GeV/c)^2 [12, 13]), factorization in meson electroproduction may still be questionable at such Q^2.

During meson electroproduction, upon absorbing the virtual photon the meson and the baryon move fast in opposite directions. It has been suggested [11] that the outgoing meson maintains a small transverse size which results in a suppression of soft interactions (multiple gluon exchange) between the meson-baryon systems moving fast in opposite directions and thereby leading to factorization. Consequently, factorization is rigorously not possible without the onset of the Color Transparency (CT) phenomenon [11]. The underlying assumption here is that in exclusive "quasielastic" hadron production the hadron is produced at small interquark distances. However, just the onset of CT is not enough, because quark transverse momentum contributions can be large at lower Q^2s which could lead to breakdown of factorization. Thus it is critical to observe the onset of CT in hadron production as a precondition to the validity of factorization.

In addition, in the last few years several authors have formally identified connection between GPDs and CT. For example, M. Burkardt and G. Miller [14] have derived the effective size of a hadron in terms of a GPDs. Since CT is a result of the reduced transverse size of the hadron, the discovery of CT would place constraints on the analytic behavior of the GPDs used to derive the effective size of hadrons. This in turn would provide testable predictions for other GPD related observables such as hadron form factors. Another example is the work by S. Liuti and S. K. Taneja's [15]. They have explored the structure of GPDs in impact parameter space to determine the characteristics of the small transverse separation component of the hadron wave-function. They have also shown that nuclei can be used as filters to map the transverse component of the hadron wavefunction and thus the discovery of CT would place exact constraints on these components and provide new insight into the GPDs which are used to calculate the wave-functions. These theoretical works show the very important link between GPDs and CT and provides additional motivation for the search for CT.

2.2 Previous Measurements

2.2.1 Proton Knockout Experiments

Several measurements of the transparency of the nuclear medium to high energy protons in quasielastic A(p,2p) and A(e,e$'$p) reactions have been carried out over the last decade. The nuclear transparency measured in A(p,2p) at Brookhaven [16] has shown a rise consistent with CT for Q$^2 \simeq$ 3 - 8 (GeV/c)^2, but decreases at higher momentum transfer. Data from a new experiment [17], completely reconstructing the final-state of the A(p,2p) reaction, confirm the surprising findings of the earlier Brookhaven experiment (see Fig. 1).

The drop in the transparency can be understood in view of similar irregularities in the energy dependence of p-p scattering for a center-of-mass angle $\theta_{cm} = 90^\circ$, and large spin effects. This has led to suggestions of the presence of interference mechanisms in

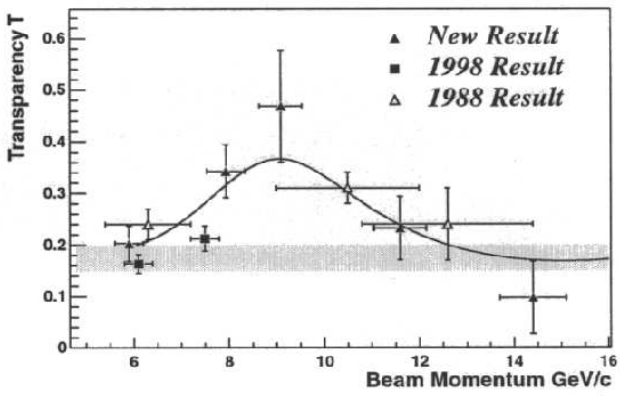

Figure 1: Nuclear transparency measured in $A(p, 2p)$ reactions [16, 17]. The shaded band is a Glauber calculation for Carbon while the solid line is a fit to a function which is proportional (but out-of-phase by π radians) to the oscillations in the $p - p$ scattering cross-section scaled by s^{10}, where s is square of the center of mass energy. This is based on the nuclear filtering idea [18].

this process [18], corresponding to an interplay between small- an large-size proton wave function configurations. The simplest solution to prevent such complications is to perform similar experiments using the clean e-p scattering process.

The A(e,e′p) measurements at SLAC [19] and at JLab [20, 21] yielded distributions in missing energy and momentum completely consistent with conventional nuclear physics predictions (as shown in Fig. 2). As an example, the high-Q^2 measured JLab ^{12}C(e,e′p) yields [21], as function of missing momentum, and the predictions from a Monte Carlo simulation are shown in Fig. 2. The requirement that the missing energy, E_m, <80 MeV was applied to both data and Monte Carlo distributions. Good agreement between the momentum distributions is observed for all Q^2 points measured. A similar good agreement is obtained between the experimental and simulated ^{12}C(e,e′p) yields as function of missing energy. The net effect of radiative corrections, for these kinematics, is a renormalization of the integrated yield, up to $E_m = 80$ MeV, by 36%.

The extracted transparencies, as shown in Fig. 3, exclude sizable CT effects up to $Q^2 = 8.1$ (GeV/c)^2, in contrast to the A(p,2p) results [16]. The measurements rule out several models predicting an early, rapid, onset of CT, but can not exclude models predicting a slow onset of CT (see Fig. 4). Therefore it is critical to extend these measurements to higher Q^2 where most CT models can be rigorously tested.

It has been predicted [25] that exclusive processes in a nuclear medium are cleaner than the corresponding processes in free space. Large quark separations may tend not to propagate significantly in the strongly interacting medium. Configurations of small quark separations, on the other hand, will propagate with small attenuation. This phenomenon is termed nuclear filtering, and is the complement of CT phenomena. If such nuclear filtering occurs, the nuclear medium should eliminate the long distance amplitudes. Thus, in the large A limit, one is left with a perturbatively calculable limit. Such nuclear filtering could, e.g., explain the apparent contradiction between the proton transparency results

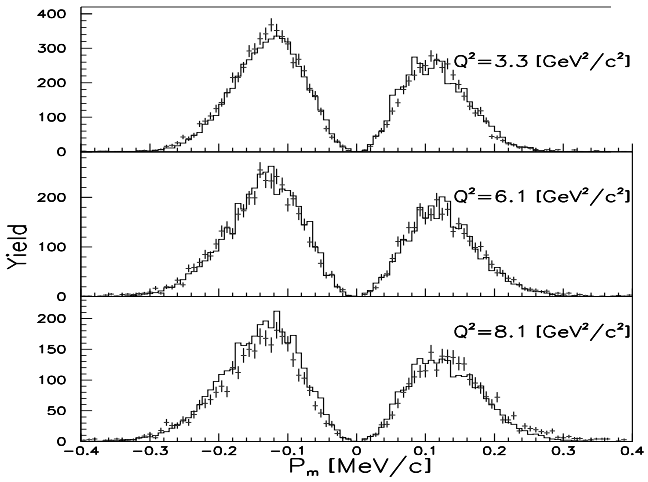

Figure 2: Experimental yield (pluses) as a function of missing momentum for the ^{12}C(e,e′p) reaction, with the hadron spectrometer positioned at the quasi-free angle, compared to simulated yields (histogram), at Q^2 = 3.3, 6.1, and 8.1 (GeV/c)^2. The data are integrated over a missing energy region up to 80 MeV. Positive (negative) missing momentum is defined as a proton angle larger (smaller) than the momentum transfer angle.

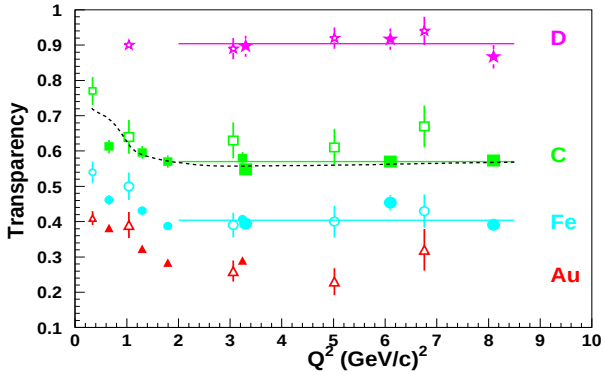

Figure 3: Nuclear transparency as a function of Q^2, for ^{2}H (stars), ^{12}C (squares), ^{56}Fe (circles) and ^{197}Au (triangles). The small open symbols are results from MIT-Bates [22], the large open symbols are results from the SLAC experiment NE-18 [19], the small solid symbols are results from the earlier JLab experiment [20] and the large solid symbols are results from the later JLab experiment [21]. The dashed line is a Glauber calculation of Pandharipande et al. [23] and the solid lines are fit to a straight line of the results for $Q^2 > 2.0$ (GeV/c)^2.

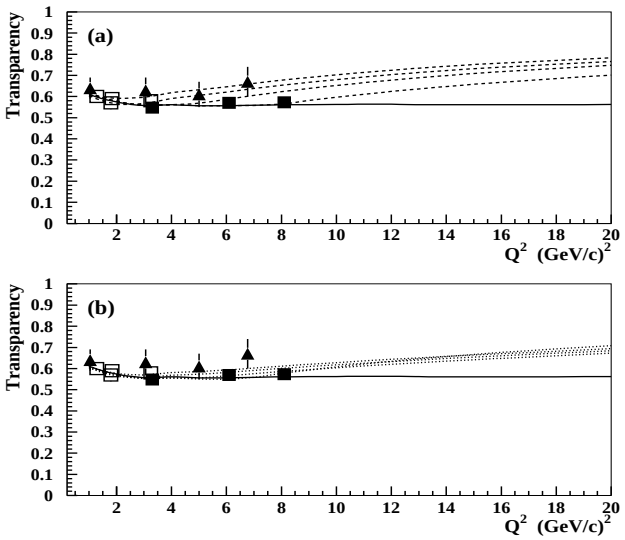

Figure 4: Nuclear transparency as a function of Q^2, for ^{12}C. The data are the same as in Fig. 3. The solid line is the prediction of the Glauber approximation. In (a) the dashed curves correspond to the CT prediction in the quantum diffusion model [24] with the parameter corresponding to the proton mass squared difference between its point-like-configuration and in its normal state, ΔM_p^2 set to 0.7 GeV^2 and the CT onset set to $Q_0^2 = 1$ (upper curve), 2, 4, 6, and 8 (GeV/c)^2 (lowest curve). In (b) the dotted curves correspond to CT predictions for ΔM_p^2 set to 1.1 GeV^2 and $Q_0^2 = 1$ (upper curve), 2, 4, 6, and 8 (GeV/c)^2 (lowest curve). All calculations have been normalized to the data at Q^2 = 2 (GeV/c)^2.

from A(p,2p) and A(e,e′p) experiments, mentioned above. The resolution [18] may be that the interference between short and long distance amplitudes in the free *p*-*p* cross section are responsible for these energy oscillations, where the nuclear medium acts as a filter for the long distance amplitudes. [Still, questions remain with the recent claim that the nuclear transparencies at $Q^2 \simeq 8$ (GeV/c)^2 in A(p,2p) experiments deviate from Glauber predictions [17]]. On the other hand the anomalous energy dependence of the A(p,2p) results can also be explained in terms of excitation of charm resonances beyond the charm production threshold in these processes [26].

With JLab upgraded to 12 GeV we can improve the experimental situation by pushing the A(e,e'p) measurements to significantly higher values of Q^2 where the CT predictions diverge appreciably from the predictions of conventional calculations (see Fig. 4). The Brookhaven data seem to establish a definite increase in nuclear transparency for nucleon momenta ≥ 7 GeV/c. Thus, A(e,e′p) measurements at $Q^2 > 12$ (GeV/c)^2, corresponding to comparable momenta of the ejected nucleon, would unambiguously answer the question whether one has entered the CT region for nucleons. This would help establish the threshold for the onset of CT phenomena in three quark hadrons. Moreover, observation of CT or lack of CT would help pick out the right explanation for the energy dependence observed in nuclear transparency from A(p,2p) experiments at BNL.

2.2.2 Meson Production Experiments

Intuitively, one expects an earlier onset of CT for meson production than for hard proton scattering, as it is much more probable to produce a small transverse size in a $q\bar{q}$ system than in a three quark system [27]. Moreover the evolution distances (formation length) are easily larger than the nuclear radius even at moderate Q^2 (the evolution time is dilated by a factor E/M in the frame of the fast moving small transverse size object, with E and M being the the energy and mass of the pion). This increases the chances of the small transverse size object to pass undisturbed through the nucleus.

Recent experiments performed at Fermilab, DESY and JLab seem to support this idea [28, 29, 30]. The first such experiment looked at the incoherent ρ^0 meson production in muon scattering from nuclei. The cross-section for these processes were parameterized as $\sigma_N = \sigma_0 A^\alpha$, where σ_0 is the hadron-N cross-section in free space. An increase in the parameter α as a function of Q^2 as observed in this experiments was interpreted as an onset of CT [31]. However, a later experiment by the HERMES collaboration [29] showed the increase in transparency to be related to the coherence length of the ρ^0 production process. More recently, the HERMES collaboration [32] has reported a positive slope, consistent with CT, in the Q^2 dependence of nuclear transparency from coherent and incoherent ρ^0 production from nuclei at fixed coherence length. Moreover, an experiment carried out at Hall-B in JLab, measuring the nuclear transparency of incoherently produced ρ^0 mesons at fixed coherence length will provide high statistics results in the near future [33].

Another such experiment is the Fermilab experiment on coherent diffractive dissociation of 500 GeV/c negative pions into di-jets [34]. The inferred Q^2 for this reaction was ≥ 7 (GeV/c)^2. The A-dependence of the data was fit assuming $\sigma \propto A^\alpha$ The alpha values were determined to be $\alpha \sim 1.6$, far larger than the $\sigma \propto A^{0.7}$ dependence typically observed in inclusive π-nucleus scattering, and the experimental results were consistent with the predicted theoretical [35] values that include CT. The authors of this experiment consider the data to have conclusively shown full CT for pions at these high momentum transfers. Of course, these data do not inform about the kinematic onset of CT.

Another recent experiment at JLab carried out the first measurement of nuclear transparency of the $\gamma n \to \pi^- p$ process on ^{4}He nuclei [37]. This experiment exploited several advantages of ^{4}He such as the relatively small size of the ^{4}He nucleus. The extracted nuclear transparency for the ^{4}He target along with calculations is shown in Fig. 5. The traditional nuclear physics calculation appears to deviate from the data at the higher energies. These data suggest the onset of deviation from traditional calculations, but future experiments with significantly improved statistical and systematic precision are essential to put these results on a firmer basis.

The most recent experiment to look for CT was also performed at JLab, where the (e,e'π^+) process on ^{1}H, ^{2}H, ^{12}C, ^{26}Al, ^{64}Cu and ^{197}Au was used to measure the pion transparency over a Q^2 range of 1 – 5 (GeV/c)^2 [38]. The nuclear transparency is extracted in this experiment by comparing the pion production from heavy nuclei to that from hydrogen. A PWIA simulation of pion-electroproduction can reproduce the shapes of the W, Q^2 and $|t|$ distributions reasonably well. For example, the W and Q^2 distributions for ^{12}C(e,e'π) (in red) are shown along with the PWIA simulation (in blue) in Fig. 6 for Q^2 between 3 – 5 (GeV/c)^2. A cut has been placed at the 2-pion production threshold

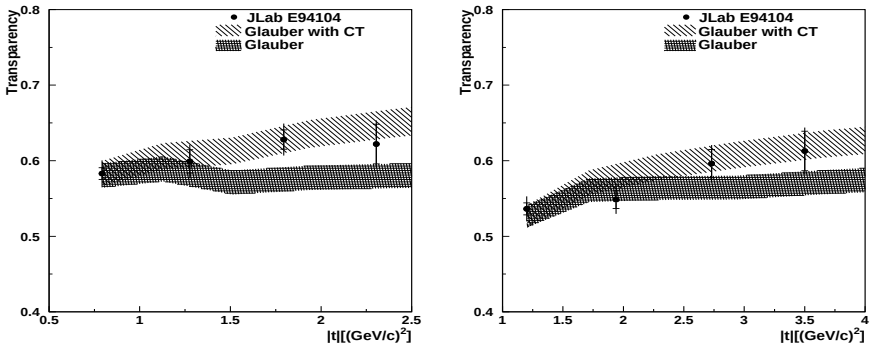

Figure 5: The nuclear transparency of ^{4}He(γ,p π^-) at θ^{π}_{cm} =70° and 90°, as a function of momentum transfer square $|t|$. The inner error bars shown are statistical uncertainties only, while the outer error bars are statistical and point-to-point systematic uncertainties (2.7%) added in quadrature. In addition there is a 4% normalization/scale systematic uncertainty which leads to a total systematic uncertainty of 4.8%.

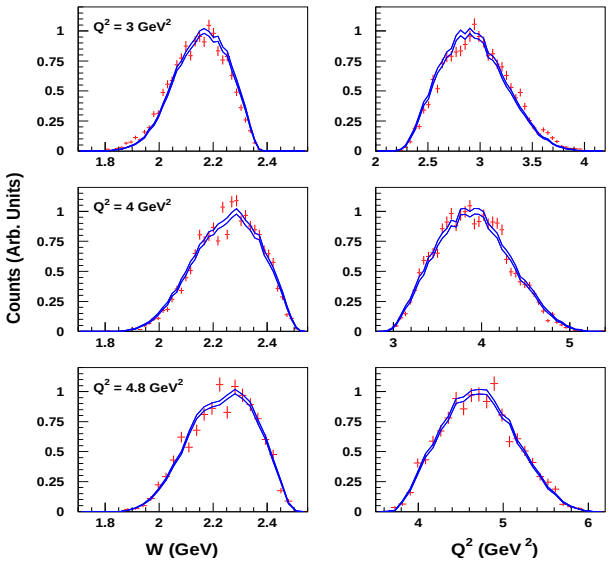

Figure 6: The W and Q^2 distributions for ^{12}C(e,e'π) (in red) compared to the PWIA simulation in blue at Q^2 = 3, 4 and 4.8 GeV^2. The statistical uncertainty only of the data and simulation are shown.

in ^{12}C. The good agreement seen in Fig 6 is typical for all targets and over the entire Q^2 range. The missing-mass spectra for ^{12}C are shown in Fig. 7, which show that the e-pion production threshold is clearly identifiable even at the highest Q^2. This gives us confidence in this experimental technique for extracting nuclear transparency from A(e,e'π^+) measurements. The preliminary results from experiment E01-107 for the Q^2 and A dependence of the transparency, hint at a CT-like effect above Q^2 of 2 (GeV/c)^2, similar to the observations of other meson production experiments mentioned earlier. We must stress here that both the Q^2 and A dependence of meson electroproduction is needed to distinguish between CT-like effect and any other reaction-mechanism related energy dependence of the transparency.

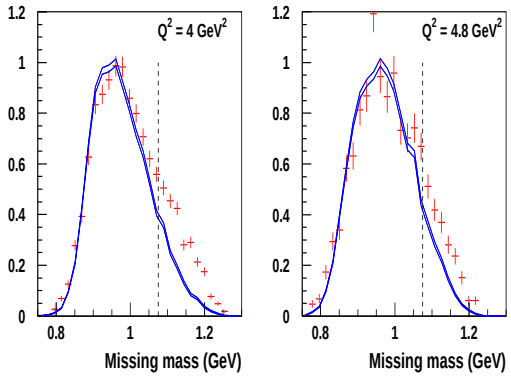

Figure 7: The missing-mass spectra for ^{12}C(e,e'π), data are shown in red while the simulation is shown in blue. The two-pion threshold is indicated by the vertical dashed line.

All these experiments suggest that the onset of CT phenomena for mesons, is most likely below $Q^2 = 10$ (GeV/c)^2. Please note that prior to the recent (e,e'π^+) experiment, the elementary pion electroproduction process was not known in detail. We prefer to view the low-Q^2 data from the E01-107 experiment to provide the first reliable "baseline" for this process. The CT effects can be unambiguously verified only as a deviation from a baseline nuclear physics calculation. A Q^2 dependence of the pion transparency in nuclei may also be introduced by conventional nuclear physics effects at the lower Q^2s. Thus one must simultaneously examine both the Q^2 and the A dependence of the meson transparency. Several independent calculations [25, 36] predict the CT effect to be largest above Q^2 of 10 (GeV/c)^2, which is in agreement with the observation of full CT in the Fermilab experiment mentioned above. Using a 11 GeV beam one can extend the (e,e'π^+) measurement on nuclear targets to Q^2 of 10 (GeV/c)^2. Thus, using the data collected for $Q^2 < 5$ (GeV/c)^2 as a baseline, the new data could help confirm and help establish the CT phenomena in mesons on a firm footing.

2.3 Summary

The suggested 12-GeV A(e,e′p) and A(e,e′π^+) experiments will allow:
1. A sensitive search for the onset of Color Transparency phenomenon in a region of Q^2 that seems optimally suited for this search.
2. The A(e,e′p) process will provide valuable information on the interpretation of the rise in nuclear transparency found by the BNL A(p,2p) experiments. This is true even if these experiments do not find any rise of nuclear transparency in the measured Q^2 range.
3. The A(e,e′π^+) process can validate the strict applicability of factorization theorems for meson electroproduction experiments.

3 The Experiment

3.1 Overview

The proposed experiment will measure the A(e,e'p) cross section on ^{1}H and ^{12}C over a Q^2 range of 8 - 16 (GeV/c)^2 and the A(e,e′π^+) cross section on ^{1}H, ^{2}H, ^{12}C and ^{63}Cu over a Q^2 range of 5 - 9.5 (GeV/c)^2. We propose to use the HMS as the electron spectrometer and the SHMS will be used to detect the final state hadron (proton or pion). The scattered electron and final state proton/pion will be detected in coincidence in quasi-free kinematics. The transparency for the A(e,e'p) process will be extracted by comparing the experimental yield from the ^{12}C targets with the yield from a Plane Wave Impulse Approximation (PWIA) simulation of the experiment. Since the PWIA simulation does not include any final state interactions, the ratio of these yields is a measure of the transparency of the target nuclei to protons. In PWIA the coincidence cross-section for a discrete transition is given by;

$$\frac{d^5\sigma}{dEd\Omega_e d\Omega_x} = k_x \sigma_{ep} S(E_m, |P_m|), \tag{1}$$

where $S(E_m, |P_m|)$ is the single particle spectral function and σ_{ep} is the off-shell e-p cross-section. In addition, the PWIA Monte Carlo simulation of the experiment includes detailed descriptions of the spectrometers, multiple scattering, ionization energy loss, and radiative effects. It uses the deForest prescription [39] for the elementary off-shell *ep* cross-section which is folded with an Independent-Particle Shell Model (IPSM) spectral functions for the given target nucleus. The ^{1}H(e,e'p) data will be used for normalization and to verify the accuracy of the Monte Carlo simulation. This is a well established technique that we have successfully used in the past (E91-013, E94-139) to extract nuclear transparencies for A(e,e'p) processes over a wide range of Q^2 and A. This experiment will extend these measurements up to the highest Q^2 easily accessible at the upgraded JLab. The standard detector packages, which include the high-pressure gas Cerenkov detector, will be sufficient for PID. The planned aerogel detector would be beneficial for kaon selection. This detector is not part of the base equipment, but is anticipated to be built with early operations funds.

For the A(e,e'π) process we will compare the yields from ^{2}H(e,e′π^+), ^{12}C(e,e′π^+) and ^{63}Cu(e,e′π^+) to the yield from ^{1}H(e,e′π^+) at identical kinematics. A Monte Carlo simulation of the experiment that includes detailed descriptions of the spectrometers, decay of

the pions in flight, multiple scattering, ionization energy loss, and radiative corrections will be used to extract the acceptance corrected yields for the A(e,e'π) process. The Monte Carlo will use a model of charged pion electroproduction from nucleons to account for variations of the cross section across the acceptance. For electroproduction from ^{2}H, ^{12}C, and ^{64}Cu, this model will be implemented in a quasifree approximation in combination with realistic spectral function. It is necessary to integrate the cross sections over the missing mass peak. In parallel kinematics, this cross section can be expressed as:

$$\int_{\Delta M_x} \frac{d\sigma}{d\Omega_\pi dM_x} = \int_{\Delta M_x} \frac{d\sigma_T}{d\Omega_\pi dM_x} + \epsilon \int_{\Delta M_x} \frac{d\sigma_L}{d\Omega_\pi dM_x}\,, \tag{2}$$

where ΔM_x is the region of missing mass within the experimental acceptance. In the case of the free proton, the missing mass is just a radiation broadened δ function at the neutron mass. For the other target nuclei, the Fermi motion of the bound nucleons broadens the distributions, and the missing mass coverage is limited by the acceptance of the spectrometers. To limit the uncertainty due to the pion electroproduction model we will take ^{1}H(e,e'π^+) data in a larger θ_{pq} and W grid than for the other nuclear targets. In addition, an iterative procedure will be used to optimize the pion electroproduction model and match the resulting Monte Carlo distributions to the data. This technique has also been successfully used before in experiment E01-107. In this part of the experiment, W will be kept > 2.1 GeV such that it is always above the resonance region, and $|t|$ will be kept below 0.5 GeV^2 to minimize final state interactions and also to keep the reaction mechanism constant while the momentum transfered to the pion is increased, at the suggestion of a previous Program Advisory Committee advising on the 6-GeV E01-107 experiment. This would help us isolate the transparency from other reaction-mechanism related effects. Moreover, by looking at both the Q^2 and A dependence of the transparency one can isolate the CT effect.

3.2 Kinematics

The quasi-free kinematics for the A(e,e'p) and A(e,e'π) processes are shown in Tables 1 and 2 respectively. These kinematics fall well within the kinematics accessible by the SHMS-HMS spectrometer pair.

Q^2	E_e	$\theta_{e'}^{HMS}$	$p_{e'}^{HMS}$	θ_p^{SHMS}	p_{SHMS}	T_p
(GeV/c)^2	GeV	deg	GeV/c	deg	GeV/c	GeV
8.0	8.8	25.90	4.531	22.73	5.122	4.27
10.0	8.8	33.30	3.465	17.86	6.203	5.36
12.0	8.8	44.30	2.400	13.32	7.278	6.40
14.0	11.0	35.00	3.525	14.00	8.360	7.47
16.4	11.0	48.05	2.251	10.00	9.642	8.75

Table 1: Kinematics for the A(e,e'p) process.

Q^2	E_e	W	t	$\theta_{e'}^{HMS}$	$E_{e'}$	θ_{π}^{SHMS}	p_π	k_π
$(GeV/c)^2$	GeV	GeV	GeV^2	deg	GeV	deg	GeV/c	GeV
5.0	11.0	2.43	-0.40	16.28	5.67	15.96	5.110	0.67
6.5	11.0	2.74	-0.40	22.13	4.010	11.72	6.771	0.67
8.0	11.0	3.02	-0.40	32.37	2.340	7.90	8.442	0.67
9.5	11.0	3.09	-0.48	47.71	1.320	5.52	9.42	0.74

Table 2: Kinematics for the A(e,e'π) process.

3.3 Electron Beam and Targets

A 80 μA CW electron beam will be used on the solid (liquid) targets. We intend to use the 15 cm long cryogenic hydrogen and deuterium targets, and Al dummy targets for window subtraction. In addition we will use 6% radiation length ^{12}C and ^{63}Cu foils. These are standard targets that are available for Hall C experiments. An existing 2.5% radiation length ^{12}C target will also be used to collect data at the lowest Q^2 in order to verify the radiative corrections procedure used in the data analysis.

3.4 The Spectrometers

The SHMS-HMS spectrometer pair will be used to perform these coincidence measurements. The HMS spectrometer will be used as the electron arm for both A(e,e'p) and A(e,e'π). The HMS momentum setting ranges from 1.32 to 5.67 GeV/c. The standard particle identification capabilities of HMS are more than sufficient to provide e^-/π^- separation for these coincidence reactions. The singles rate in the HMS will be less than 100KHz, well within the acceptable range for HMS.

The SHMS will be used as the hadron arm in this experiment and its momentum setting will range from 5.11 to 9.64 GeV/c. Adequate $p/K^+/\pi^+$ separation will be achieved in the SHMS using the combination of heavy gas Cerenkov and aerogel Cerenkov detectors [40], as per their expected performance shown in Fig. 8. The singles rate in the SHMS will be less than 100KHz, well within the SHMS design parameters.

3.5 Counting Rates

The counting rate were estimated using a Monte Carlo simulation of the experiment using the Hall C Monte Carlo SIMC. The A(e,e'p) cross-section is calculated using a PWIA model which folds the elementary off-shell $e-p$ elastic cross-section with a spectral function for the target nuclei and the two spectrometer acceptance models. A constant nuclear transparency, consistent with previous results, is taken into account. The coincidence rates are shown in Table 3 and singles rates as well as the signal to noise ratio are shown in Table 4. The singles pion and proton rates were estimated using the the parametrization of SLAC data of Wiser *et al.* [41]. The electron singles rates were estimated using the code QFS [42]. A coincidence timing window of 2 ns was used in the estimation of the accidental rates.

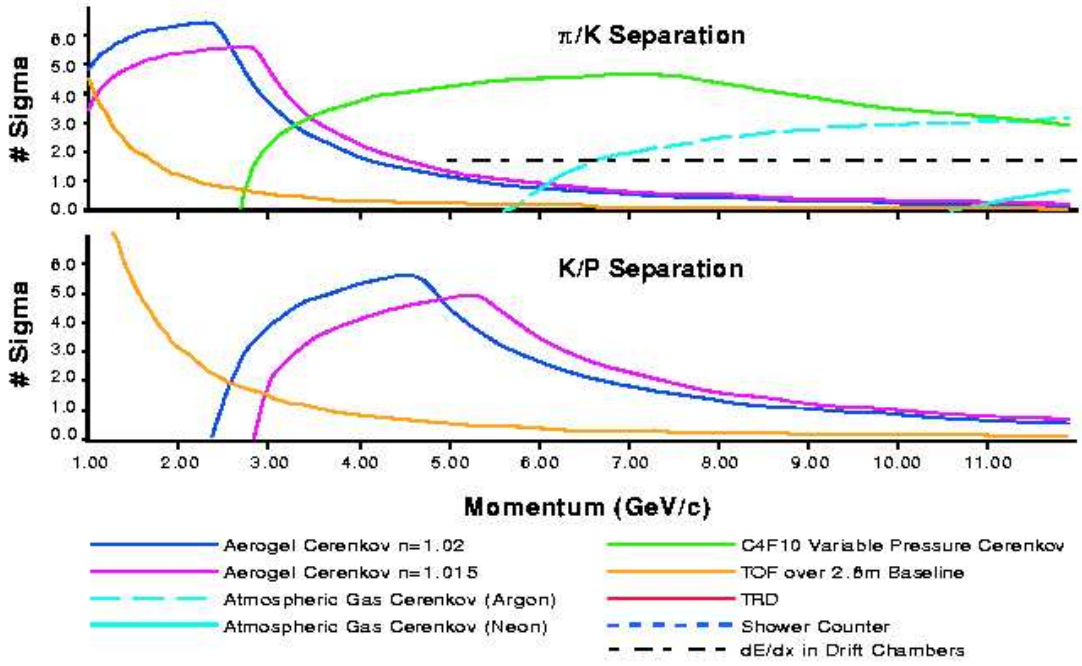

Figure 8: The expected hadron PID with the SHMS detectors.

The H(e,e'π) rates were similarly calculated using the Hall-C Monte Carlo package SIMC, which folds the elementary pion-electroproduction cross-section with a detailed model of the two spectrometer acceptance. The electro-pion production cross-section from a nucleon is a parametrization of the data from Brauel *et al* [43]. For the A(e,e'π) reaction, rates were calculated by multiplying the H(e,e'π) with a figure of merit (FOM) for each target (see Table 6). The FOM is defined as: $t/A \times Z \times T$, with t the target thickness in g/cm^2, A the nucleon number, Z the proton number (as exclusive π^+ electroproduction only occurs off the protons), and T an estimated pion transparency number based upon the values measured at lower Q^2.

A 80 μA beam was assumed for all targets. The estimated coincidence rates, singles rates and the signal to noise are shown in Table 5. The singles pion and proton rates were again estimated using the parameterization of SLAC data of Wiser *et al.* [41], and the electron singles rates with [42] and the fit by Bodek *et al.* of the DIS region, folded with the nuclear EMC effect. We again assumed a coincidence timing resolution of 2 ns in the estimation of the accidental rates. The main source of background in these experiments are the single electron and π/proton rates in each spectrometer and the accidental coincidences due to these singles events. However, the signal-to-noise is easily adequate to allow background subtraction during data analysis.

3.6 Beam Time Estimate

The beam time estimates for a 2% statistical uncertainty are shown in Tables 7 and 8. The estimates include the extra time for collecting ^{1}H(e,e'π^+) data over a larger range of θ_{pq}, and also the time to use a 2.5% radiation lenght Carbon target to verify the (external)

Q^2	H(e,e'p) Rate	^{12}C(e,e'p) Rate
(GeV/c)^2	/hr	/hr
8.0	8942	2446
10.0	1801	527
12.0	337	109
14.0	278	87
16.4	50	17

Table 3: The coincidence rates for the ^{1}H(e,e'p)and ^{12}C(e,e'p) reactions, assuming 2% radiation length cryogenic and 6% radiation length solid targets and 80 μA beam currents.

Q^2	Singles (h arm)		Singles (e arm)		S/N
(GeV/c)^2	KHz	KHz	Hz	KHz	$\times 10^3$
	p	π^+	e	π^-	
8.0	1.0	1.2	58.7	0.5	5.8
10.0	1.3	1.4	10.8	1.2	4.7
12.0	2.4	2.6	1.9	3.8	1.1
14.0	4.5	4.2	2.7	4.2	0.4
16.4	6.2	12.2	0.5	5.5	0.06

Table 4: Singles rates and signal-to-noise for ^{12}C(e,e'p) (6% target and 80μA current). The signal-to-noise is given by coin rate/(singles rate (e + π^-/1000) $\times$ singles rate (p + π^+/1000)$\times$ 2 ns).

Q^2	Coinc rate (^{1}H)	Singles (^{12}C)(h arm)		Singles (^{12}C) (e arm)		S/N
(GeV/c)^2	/hr	π^+ KHz	p KHz	e KHz	π^- KHz	
5.0	4930.6	8.9	3.7	25.0	1.9	6.4
6.5	1175.0	7.0	7.8	3.0	4.3	5.6
8.0	213.1	12.2	13.4	1.1	23.7	1.8
9.5	32.8	31.2	20.0	0.07	113.2	1.6

Table 5: Coincidence rates for ^{1}H target, singles rates for ^{12}C target and signal-to-noise given by coin rate/(singles rate (e + π^-/1000) $\times$ singles rate (p + π^+/1000)$\times$ 2 ns), for the A(e,e'π) reaction.

Target	Thickness rl (%)	FOM	Run time to LH_2 time
H	2.0	1.07	1.0
D	2.0	1.09	1.0
C	6.0	0.89	1.2
Cu	6.0	0.21	5.0

Table 6: Assumed target thicknesses and derived FOM's (see text) for the quasifree A(e,e′π^+)n(A-1) reaction. The last column represents the ratio of beam time required for the nuclear targets, normalized to the ^{1}H(e,e′π^+)n case, to obtain the desired statistical uncertainty of 2%.

Q^2 (GeV/c)^2	Stat. Uncertainty %	Run time (^{1}H) (hours)	Run time (^{12}C) (hours)	Run time (total) (hours)
8.0	1	2	4+10	16
10.0	2	2	5	7
12.0	2	8	23	31
14.0	2.5	8	23	31
16.0	2.5	32	94	126
		Total		211

Table 7: Run time and statistical uncertainty for the (e,e'p) process, the additional time shown for the ^{12}C target at the lowest Q^2 is on a 2.5% radiation length target and will be used to verify the radiative correction procedure.

Q^2 (GeV/c)^2	Uncertainty %	^{1}H Run time (hours)	^{2}H Run time (hours)	^{12}C Run time (hours)	^{63}Cu Run time (hours)	Run time (total)
5.0	1	2x3	2	2.5+6	10	26.5
6.5	2	2.5x3	2.5	3+7	12.5	32.5
8.0	3	5x2	5	6	25	46.0
9.5	3	34x2	34	41	170.0	313.0
				Total		418

Table 8: Run time and statistical uncertainty for the (e,e'π) process. The additional time for the ^{1}H target is to cover larger θ_{pq} around the parallel kinematics. The additional time on the ^{12}C target at the lowest 2 Q^2 points is on a 2.5% radiation length target and will be used to test the radiative correction procedure.

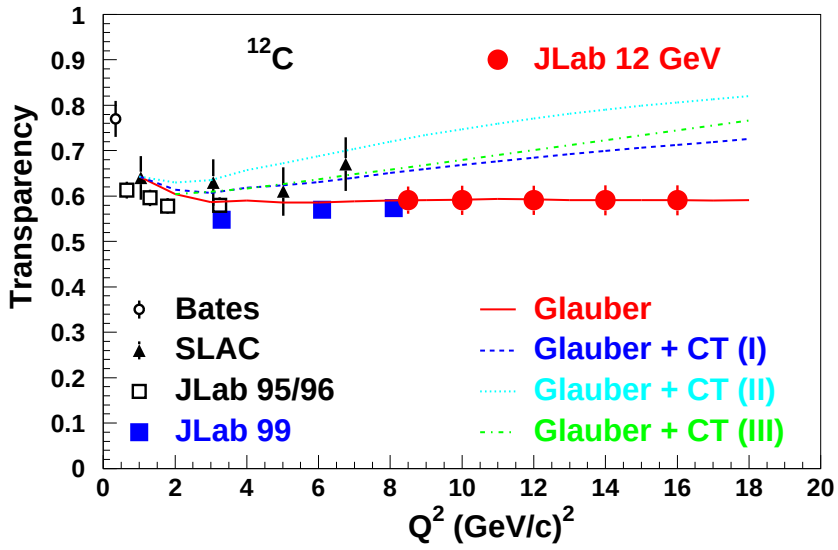

Figure 9: The projected results for ^{12}C(e,e'p) along with all previous measurements. The error bars represent the quadrature sum of the statistical and the a 5% systematic uncertainty. Also shown are the predictions of various CT calculation, CT(I) [44], CT(II) [45], CT(III) [46] and also a traditional calculation without CT [23].

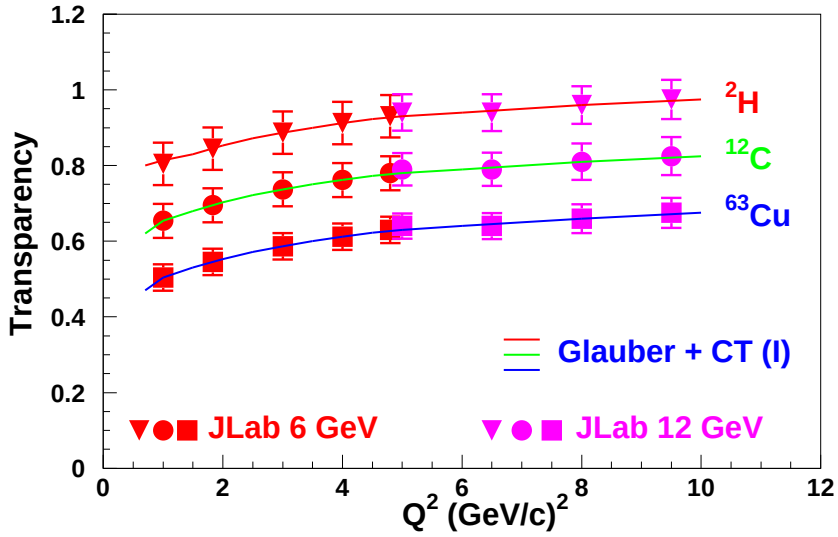

Figure 10: The projected results for A(e,e'π) along with all projections from E01-107. The error bars represent the quadrature sum of the statistical and the a 5% systematic uncertainty. Also shown are the CT calculations of Ref. [44].

radiative correction procedure. A total of 629 hours (∼26 days) is requested. Projected results are shown in Figs. 9 and 10, along with previous results for the A(e,e′p) reaction. Preliminary results for the A(e,e′π^+) reaction, from the E01-107 experiment, will be shown during the PAC presentation.

References

[1] A.H. Mueller, in Proceedings of the Seventeenth Recontre de Moriond Conference on Elementary Particle Physics, Les Arcs, France, 1982, edited by J. Tran Thanh Van (Editions Frontieres, Gif-sur-Yvette, France,1982); S.J.Brodsky, in Proceedings of the Thirteenth International Symposium on Multiparticle Dynamics, Volendam, The Netherlands, 1982, edited by W. Kittel et al. (World Scientific, Singapore, 1983).

[2] D. Perkins, Phil. Mag. **46**, 1146 (1955).

[3] L.L. Frankfurt, G.A. Miller, and M.I. Strikman, Comments Nucl. Part. Phys. **21**, 1 (1992).

[4] S.J. Brodsky, L. Frankfurt, J.F. Gunion, A.H. Mueller, and M. Strikman, Phys. Rev. D **50**, 3134 (1994).

[5] J. Collins, L. Frankfurt, and M. Strikman, Phys. Rev. D **56**, 2982 (1997).

[6] L.L. Frankfurt, P.V. Pobylitsa, M.V. Polyakov, and M. Strikman, Phys. Rev. D **60**, 014010 (1999).

[7] M. Diehl, T. Gousset, B. Pire, and O. Teryaev, Phys. Rev. Lett. **81**, 1782 (1998).

[8] X. Ji, Phys. Rev. Lett. **78**, 610 (1997); Phys. Rev. D **55**, 7114 (1997).

[9] A.V. Radyushkin, Phys. Lett. **B380**, 417 (1996); Phys. Rev. D **56**, 5524 (1997).

[10] M. Eides, L. Frankfurt, and M. Strikman, Phys. Rev. D **59**, 114025 (1999).

[11] M. Strikman, Nucl. Phys. **A663&A664**, 64c (2000).

[12] M. Vanderhaeghen, P.A.M. Guichon, and M. Guidal, Phys. Rev. D **60**, 094017 (1999).

[13] A. Airapetian *et al.*, Eur. Phys. Jour. C **17**, 389 (2000).

[14] M. Burkardt and G. Miller (hep-ph/0312190)

[15] S. Liuti and S. K. Taneja, PRD **70**, 07419 (2004).

[16] A.S. Carroll *et al.*, Phys. Rev. Lett. **61**, 1698 (1988).

[17] Y. Mardor *et al.*, Phys. Rev. Lett. **81**, 5085 (1998); A. Leksanov *et al.*, hep-ex/0101039 (2001).

[18] J.P. Ralston and B. Pire, Phys. Rev. Lett. **61**, (1988), 1823; J.P. Ralston and B. Pire, Phys. Rev. Lett. **65**, (1990), 2343

[19] N.C.R. Makins *et al.*, Phys. Rev. Lett. **72**, 1986 (1994); T.G. O'Neill *et al.*, Phys. Lett. **351**, 87 (1995).

[20] D. Abbott *et al.*, Phys. Rev. Lett. **80**, 5072 (1998).

[21] K. Garrow *et al.*, Phys. Rev. C **66**, 044613 (2002).

[22] G. Garino *et al.* Phys. Rev. C **45**, (1992), 780.

[23] V. R. Pandharipande and S. C. Pieper, Phys. Rev. C **45**,(1992), 791; H. Gao, V. R. Pandharipande and S. C. Pieper (private communication).

[24] G. R. Farrar, H. Liu, L.L. Frankfurt, and M.I. Strikman, Phys. Rev. Lett. **61**, 686 (1988).

[25] B. Kundu, J. Samuelsson, P. Jain, and J.P. Ralston, Phys. Rev. D **62**, 113009 (2000).

[26] S. J. Brodsky, and G. F. de Teramond,Phys. Rev. Lett. **60**, 1924 (1988).

[27] B. Blattel ét al., Phys. Rev. Lett. **70**,(1993), 896.

[28] E. M. Aitala *et al.*, Phys. Rev. Lett. **86**, (2001),4773.

[29] R. Akerstaff *et al.*, Phys. Rev. Lett. **82**, (1999), 3025.

[30] D. Dutta *et al.*, Phys. Rev. C **68**, (2003), 021001R.

[31] M. R. Adams *et al.*, Phys. Rev. Lett. **74**, (1995), 1525.

[32] A. Airapetian *et al.*, Phys. Rev. Lett. **90**, (2003),052501.

[33] K. Hafidi *et al.*, Q^2 Dependence of Nuclear Transparency for Incoherent ρ^0 Electroproduction, Jefferson Lab Proposal E02-110.

[34] E.M. Aitala *et al.*, hep-ex/0010044 (2000).

[35] L.L. Frankfurt, G.A. Miller, and M.I. Strikman, Phys. Lett. **B304**, 1 (1993).

[36] G. Miller, in *Proc. Workshop on Options for Color Coherence/Transparency Studies at CEBAF*, CEBAF, Newport News, May 22-23 (1995).

[37] H. Gao and R. Holt *et al.* Proposal for JLab experiment E94-104 (unpublished).

[38] D. Dutta, R. Ent, K. Garrow *et al.* Proposal for JLab experiment E01-107 (unpublished).

[39] T. de Forest Jr., Nucl. Phys. **A392**, 232 (1983).

[40] SHMS Conceptual design report (unpublished).

[41] L. W. Whitlow, SLAC-Report-357,(1990); D. E .Wiser, Ph. D. Thesis, University of Wisconsin (1977); P. Bosted private communication.

[42] J. W. Lightbody Jr. and J. S. O'Connell, NBS

[43] Brauel *et al.*, Z.Phys.C. 3(1979)101.

[44] B. Kundu *et al.*, Phys. Rev. **D 62**, (2000), 113009.

[45] L. L. Frankfurt, M. I. Strikman and M. B. Zhalov, Phys. Rev. C **50**, (1994), 2189.

[46] N. N. Nikolaev *et al.*, Phys. Rev. C **50**, (1994), R1296.

[47] A. Larson,G. Miller and M. Strikman, nuc-th/0604022.